Predictive modelling of the distribution of *Clematis* sect. *Fruticella s*. *str*. under climate change reveals a range expansion during the Last Glacial Maximum

Mingyu Li [Equal first author, 1] , **Jian He** [Equal first author, 1] , **Zhe Zhao** [1] , **Rudan Lyu** [1] , **Min Yao** [1] , **Jin Cheng** [Corresp., 1] , **Lei Xie** [Corresp. 1]

[1] Beijing Forestry University, Beijing, China

Corresponding Authors: Jin Cheng, Lei Xie
Email address: chengjin@bjfu.edu.cn, xielei@bjfu.edu.cn

Background. The knowledge of distributional dynamics of living organisms is a prerequisite for protecting biodiversity and for the sustainable use of biotic resources. *Clematis* sect. *Fruticella s*. *str*. is a small group of shrubby, yellow-flowered species distributed mainly in arid and semi-arid areas of China. Plants in this section are both horticulturally and ecologically important.

Methods. Using past, present, and future environmental variables and data with Maximum Entropy (Maxent) modeling, we evaluated the importance of the environmental variables on the section's estimated distributions, thus simulating its distributional dynamics over time. The contractions and expansions of suitable habitat between the past and future scenarios and the present were then compared.

Results and Discussion. The models revealed that the areas with high and moderate suitability currently encompass about 725,110 km^2. The distribution centroid location varies between points in Ningxia and Inner Mongolia during the different scenarios. Elevation, Mean UV-B of Lowest Month, Precipitation of Coldest Quarter, and Mean Temperature of Driest Quarter were major factors determining the section's distribution. Our modeling indicated that *Clematis* sect. *Fruticella* underwent a significant range contraction during the last interglacial period, and then expanded during the last glacial maximum (LGM) to amounts like those of the present. Cold, dry, and relatively stable climate, as well as steppe or desert steppe environments may have facilitated range expansion of this cold-adapted, drought-resistant plant taxon during the LGM. Predicted future scenarios show little change in the amounts of suitable habitat for *Clematis* sect. *Fruticella*. This study aids understanding of the distributional dynamics of *Clematis* sect. *Fruticella*, and the results will help the conservation and sustainable use of these important woody plants in Chinese arid and semiarid areas.

1 **Predictive modelling of the distribution of *Clematis***

2 **sect. *Fruticella s. str*. under climate change reveals a**

3 **range expansion during the Last Glacial Maximum**

5 Mingyu Li, Jian He, Zhe Zhao, Rudan Lyu, Min Yao, Jin Cheng, Lei Xie

7 Beijing Forestry University, Beijing, PR China

9 Corresponding Author:

10 Jin Cheng, Lei Xie

11 No. 35, Tsinghua East Road, Haidian District, Beijing, 100083, China

12 Email address: chengj@bjfu.edu.cn (J. Cheng); xielei@bjfu.edu.cn (L. Xie)

15   **Abstract**

16   **Background.** The knowledge of distributional dynamics of living organisms is a prerequisite for

17   protecting biodiversity and for the sustainable use of biotic resources. *Clematis* sect. *Fruticella s.*

18   *str.* is a small group of shrubby, yellow-flowered species distributed mainly in arid and semi-arid

19   areas of China. Plants in this section are both horticulturally and ecologically important.

20   **Methods.** Using past, present, and future environmental variables and data with Maximum

21   Entropy (Maxent) modeling, we evaluated the importance of the environmental variables on the

22   section's estimated distributions, thus simulating its distributional dynamics over time. The

23   contractions and expansions of suitable habitat between the past and future scenarios and the

24   present were then compared.

25   **Results and Discussion.** The models revealed that the areas with high and moderate suitability

26   currently encompass about 725,110 km^2. The distribution centroid location varies between points

27   in Ningxia and Inner Mongolia during the different scenarios. Elevation, Mean UV-B of Lowest

28   Month, Precipitation of Coldest Quarter, and Mean Temperature of Driest Quarter were major

29   factors determining the section's distribution. Our modeling indicated that *Clematis* sect.

30   *Fruticella* underwent a significant range contraction during the last interglacial period, and then

31   expanded during the last glacial maximum (LGM) to amounts like those of the present. Cold,

32   dry, and relatively stable climate, as well as steppe or desert steppe environments may have

33   facilitated range expansion of this cold-adapted, drought-resistant plant taxon during the LGM.

34   Predicted future scenarios show little change in the amounts of suitable habitat for *Clematis* sect.

35   *Fruticella*. This study aids understanding of the distributional dynamics of *Clematis* sect.

36   *Fruticella*, and the results will help the conservation and sustainable use of these important

37   woody plants in Chinese arid and semiarid areas.

38

39   **Introduction**

40   Ecological habitats and distributions of living organisms, community compositions,

41   ecosystem structures, and global biodiversity have been significantly influenced by climate

42   changes during the Quaternary period (Qiu, Fu & Comes, 2011; Doxford & Freckleton, 2012;

43   Pio et al., 2014; Carvalho et al., 2015; Sun et al., 2015; Matías et al., 2017; Qin et al., 2017;

44   Zhang et al., 2018; Wang et al., 2019; Mohammadi et al., 2019). During the last glaciation,

45   global temperature was 5–12 ℃ lower than they are now and the glacier areas were 8.4 times of

46   the present time in China (Wang & Liu, 2001; Li et al., 2004; Chen, Kang & Liu, 2011). This

47   greatly affected plant distributions and many plant species significantly shrank their habitat

48   during that time (Xu et al., 2017; Li et al., 2019). Furthermore, the ongoing changing climate of

49   the past few decades has also been affecting living systems and the geographic distributions of

50   organisms (Parmesan & Yohe, 2003), and resolving the relationships between vegetation and

51   climate dynamics has been a critical issue of ecology study (Bellard et al., 2012). The Fifth

52   Assessment Report of the Intergovernmental Panel on Climate Change (IPCC) estimated that by

53   the end of the 21th century, average global temperatures will have increased by 0.3–4.5 ℃ as

54   greenhouse gas emissions continue to increase (IPCC, 2013). This will have major effects on

55   future ecosystems and species distributions (Walck et al., 2011; Wang et al., 2019; Li et al.,

56   2019). Distribution ranges of many plant species in the Northern Hemisphere may shift

57   northward or to higher elevations in response to the future climate changes (Hof et al., 2011; Bai,

58   Wei & Li, 2018; Wang et al., 2019; Zhang, Zhang & Tao, 2019).

59   Modeling the effects of climate change on the past and present habitats of different species

60   across a landscape aids in understanding the organisms' potential responses to their changing

61   environments going forward (Wang et al., 2019; Li et al., 2019; Zhang, Zhang & Tao, 2019).

62   Species distribution modeling (SDM) is widely used and has become a valuable tool for

63   predicting species habitat suitability (Barbet-Massin et al., 2012; Miller, 2012; Zhang et al.,

64   2012; Li & Wang, 2013). With the availability of massive digitalized specimen records and high-

65   resolution environmental data, SDM is widely used to assess current potential geographical

66   habitats and evaluate the effects of climate change in recent years (Konowalik, Prońków &

67   Prońków, 2017; Wang et al., 2018; Li et al., 2019). To accomplish such analyses, many

68   algorithms have been developed in the past decades, such as DOMAIN (Carpenter, Gillison &

69   Winter, 1993), Maximum Entropy algorithm (Maxent) (Phillips, Anderson & Schapire, 2006),

70   Generalized Linear Model (GLM) (Hirzel, Helfer & Metral, 2001), and the Generalized Additive

71   Model (GAM) (Austin et al., 2009). Of all these models, Maxent has been a powerful tool and

72   commonly used to assess the impacts of environmental factors on the suitable habitat of a given

73   taxon (Hernandez et al., 2006; Bai, Wei & Li, 2018; Li et al., 2019).

74   Drylands, including arid, semi-arid, and dry sub-humid ecosystems, constitute one of the

75   earth's largest terrestrial biomes. They cover 41% of the earth's surface and support 38% of the

76   global human population (Maestre et al., 2012). In China, drylands cover approximately 50% of

77   the total land surface, and desertification has increased rapidly in recent years. A recent study

78   discovered that semi-arid regions that dominate the drylands in northern China have experienced

79   much warming and significant expansion over the last 60 years (Huang et al., 2019). Because

80   these regions (especially in the Loess Plateau of northern China) have suffered from overgrazing,

81   subsistence farming, deforestation, and severe water loss and soil erosion, the ecosystems in

82   these regions are highly vulnerable to effects rooted in the current global climate changes (Jiang

83   et al., 2013; Liu et al., 2013). Thus, the knowledge of the distributional shifts of dryland

84   vegetation responding to climate change in that area is urgently needed to aid conservation and

85   sustainability of its biodiversity.

86   *Clematis* sect. *Fruticella s. str.* (Ranunculaceae), consisting of several erect, shrubby species

87   that grow mainly on the Loess Plateau and in the northern Hengduan Mountains, is one of the

88   most important plant taxa in northern China's arid and semi-arid ecosystems (He, Liu & Xie,

89   2018). Previous classifications broadly included all the shrubby *Clematis* species in this section

90   (Prantl, 1888; Handel-Mazzetti, 1939; Tamura, 1967, 1995; Chang, 1980; Johnson, 1997; Grey-

91   Wilson, 2000). However, the most recent taxonomic revisions (Wang, 2003; Wang & Li, 2005a,

92   2005b) considered that this broadly define section may not be a natural group due to its

93   diversified floral traits. So, they re-defined this section to include only five species with yellow,

94   bell-shaped flowers. Because of their white, spreading flowers, other, previously included,

95   shrubby species (*C. lancifolia*, *C. delavayi*, *C. ispahanica*, *C. songarica*, and *C. phlebantha*),

96   were excluded (Wang, 2003; Wang & Li, 2005b). Although the recent molecular phylogenetic

97   studies did not include all of the *Clematis* sect. *Fruticella* member species, yellow-flowered *C.*

98   *fruticosa* was found to be distantly related to white-flowered *C. delavayi* and *C. ispahanica*

99   (Lehtonen, Christenhusz & Falck, 2016), thus supporting the exclusion of the white-flowered

100 species from the section.

101 According to the current taxonomic revision, *Clematis* sect. *Fruticella s. str.* (hereinafter

102 inclusive) contains *C. fruticosa*, *C. tomentella*, *C. canescens*, *C. nannophylla*, and *C. viridis*

103 (Wang, 2003; Wang & Li, 2005a, 2005b). The former four species are found in the vast arid and

104 semi-arid areas of the Loess Plateau of northern China, and some populations extend to the Gobi

105 of Mongolia. The latter species, *C. viridis*, grows on the windy and arid slopes of north

106 Hengduan Mountains (Figure 1) and the uppermost Yangtze River's valley. Unlike most of the

107 other climbing species of *Clematis*, sect. *Fruticella* has strikingly different characteristics.

108   Besides being erect shrubs, the species' well-branched woody stems often have simple and

109   reduced leaves, specialized adaptations that minimize water loss in their arid and semi-arid

110   habitats. Plants of *Clematis* sect. *Fruticella* are cold and drought resistant and heliophilous. The

111   pollination system of this section is obligate out-crossing but self-compatible. The major

112   pollinators are *Amegill aparhypate* and *Apis cerana* (Hou et al., 2016).

113   Plants in *Clematis* sect. *Fruticella* play important roles in the dryland ecosystems in northern

114   China and have great horticultural value. *Clematis fruticosa* and *C. nannophylla* are typical

115   vegetation components of Chinese Loess Plateau and are often used in raised bed and rock

116   garden landscapes (Grey-Wilson, 2000). Because of its drought resistance and easy propagation,

117   *C. tomentella*, along with *Hedysarum scoparium*, *Caragana korshinskii*, *Calligonum*

118   *mongolicum*, and other xerophytic species, was used in straw checkerboard barriers constructed

119   to stabilize sand in the National Nature Reserves in Ningxia Province (Guo et al., 2012; Ding et

120   al., 2013). With its excellent stress tolerance, *Clematis fruticosa* would also be a good candidate

121   for sand fixing and afforestation (Liu et al., 2016).

122   However, previous studies have focused mainly on the drought-resistance and horticultural

123   utility of this section (Guo et al., 2012; Ding et al., 2013; Liu et al., 2016). Few studies have

124   examined the habitat and ecological factors that contribute to its past, current, and future

125   distribution under climate changes. Expansion and contraction of its range during Quaternary

126   glaciations may provide a forecast of future distributional fluctuations under climate change and

127   show key habitat suitability factors that are crucial for maintaining its utility and for management

128   planning. In this study, we propose hypotheses that during the Last Glacial Maximum (LGM) the

129   distribution area of *Clematis* sect. *Fruticella* was the smaller than that of the current, and in the

130   future the distribution centroid of this section will move northward or higher elevation in

131   response to global warming.

132   The ecological niche modeling (ENM) analysis is typically performed for single species.

133   Only a few studies performed ENM analysis at higher taxonomic levels, e.g. for the willow

134   family (Salicaceae) as a whole (Li et al., 2019). The present study used ENM to simulate the

135   potential distribution of *Clematis* sect. *Fruticella* for the following reasons: (1) The five species

136   are closely related and share a similar climatic niche on a larger spatial scale. As emphasized by

137   Li et al. (2019), one premise of ENM is that the ecological requirements and distributions of

138   species are in equilibrium (Peterson et al., 2011). All the members of *Clematis* sect. *Fruticella*

139   are important vegetation components in dryland of China. The habitat is unique in the genus

140   *Clematis* and even in Ranunculaceae (Wang & Li, 2005a; He, Liu & Xie, 2018); (2) The

141   accuracy of specimen identification is crucial for robust niche modeling and will greatly affect

142   the simulation results. The five species of *Clematis* sect. *Fruticella* are so closely related and

143   similar morphologically that the species identification within this section are problematic in all

144   the available online databases. For example, we can obtain 125 specimen records under the name

145   *Clematis canescens* in Chinese Virtual Herbarium (CVH, http://www.cvh.org.cn). However, more

146   than 90% of the specimens are misidentified according to the most current taxonomic revision

147   (Wang & Li, 2005a). Most of the 125 specimens are actually *C. tomentella*, some of them are *C.*

148   *viridis* and *C. fruticosa*. The distribution data is likely biased by incorrectly identified species,

149   whereas the identification at the section level is far less prone to mis-identifications. In this case,

150   we can consider *Clematis* sect. *Fruticella* as a species aggregate. (3) We combined the

151   occurrence data of *Clematis* sect. *Fruticella* so the ENM results were able to fully convey this

152   section's geographical distribution patterns.

153   In the present study, we obtained a comprehensive occurrence dataset of *Clematis* sect.

154   *Fruticella*, as well as high-resolution environmental data of its distribution areas in China and

155   Mongolia. We used that data in Maxent to build species distribution models to project and

156   quantify *Clematis* sect. *Fruticella* habitat changes under a variety of past, present, and future

157   climate scenarios to determine what influences the distributional and ecological patterns of this

158   group of plants. Our results offer a reference to assist in conservation and sustainable utility of

159   shrubby *Clematis* resources for afforestation in the drylands of China.

160

161   **Materials & Methods**

162   ***Spatial Data Compilation***

163   *Clematis* sect. *Fruticella* is distributed mainly in northern China, with one species (*C. viridis*)

164   distributed in the north Hengduan Mountains and some populations of *C. fruticosa* and *C.*

165   *canescens* occurring in Mongolia. In those areas, the annual precipitation of 110–750 mm is lowest

166   in the north and increases going southward, as does the annual average temperature of -2 to 10 °C.

167   Precipitation also decreases from the east to the west. Vegetation types are alpine shrub grassland

168   along river valleys for *C. canescens*, and desert shrub grassland and desert grassland for the other

169   species.

170   From July 2015 to May 2019, we conducted several multisite surveys for *Clematis* sect.

171   *Fruticella* across its whole distribution area, including eastern Qinghai, northwest Sichuan, western

172   Gansu, Ningxia, Shanxi, Inner Mongolia, and Hebei provinces. Our distribution data were then

173   compiled from both our field data and the CVH online database. Two other online databases, the

174   Global Biodiversity Information Facility (http://www.gbif.org; GBIF Occurrence Download,

175   https://doi.org/10.15468/dl.nuge5a) and the National Specimen Information Infrastructure of China

176   (http://www.nsii.org.cn), were also consulted. We carefully checked the distribution records and

177   identified specimens according to the current taxonomic revision (Wang & Li, 2005a). Distribution

178   records without geographic coordinates were assigned coordinates using Google Earth

179   (http://www.google.com/earth). Duplicates were removed from our analyses. Eight distribution

180   sites for *C. canescens*, 19 for *C. viridis*, 29 for *C. tomentella*, 43 for *C. nannophylla*, and 101 for *C.*

181   *fruticosa* were documented. In total, 200 records of *Clematis* sect. *Fruticella* were used in our

182   analysis (Table S1).

183   ***Environmental Variables***

184   **Current Environmental Scenario**

185   Plants of *Clematis* sect. *Fruticella* are cold and drought resistant and heliophilous. The growth

186   and reproduction of this section may have been determined by various interacting factors, such as

187   temperature, precipitation, solar radiation, and soil (Zhen & Liu, 2010; Liu et al., 2014; Yu et al.,

188   2018; He, Liu & Xie, 2018). Therefore, in this study, 35 environmental variables, including

189   climate, soil, UV-B radiation, and topography, were chosen for niche modeling analysis. We

190   obtained 19 bioclimatic variables with 2.5' spatial resolution (also referred to as 5 km^2 spatial

191   resolution) from WorldClim-Global Climate Data (http://www.worldclim.org/bioclim) (Hijmans et

192   al., 2005) and applied them to current, past, and future conditions. We also downloaded four

193   datasets (Wet days (wet), Ground frost frequency (frs), Water vapor (vap), and Cloud cover (cld))

194   from the IPCC (http://www.ipcc-data.org/observ/clim/cru_ts2_1.html) (Mitchell & Jones, 2005).

195   Six UV variables (Annual Mean UV-B (UVB1), UV-B Seasonality (UVB2), Mean UV-B of

196   Highest Month (UVB3), Mean UV-B of lowest Month (UVB4), Sum of Monthly Mean UV-B

197   during Highest Quarter (UVB5), and Sum of Monthly Mean UV-B during Lowest Quarter (UVB6)

198   were obtained from gIUV, a global UV-B radiation dataset for macroecological studies

199   (https://www.ufz.de/gluv/index.php?en=32435) (Beckmann et al., 2014). Growing degree days,

200   soil pH, and soil organic carbon were acquired from the University of Wisconsin

201   (http://nelson.wisc.edu/sage/data-and-models/atlas/maps.php) (New, Hulme & Jones, 1999) and

202   three other variables: barren/very sparsely vegetated land (NVG), mapped water bodies, and global

203   elevation (GloElev) were downloaded from the Food and Agriculture Organization (ILASA &

204   FAO, 2012). All these environmental variables were transferred into ASCII format using ArcGIS

205   10.2 Conversion Tools and then overlapped with map of Asia that was obtained from the Database

206   of Global Administrative Areas (https://www.gadm.org/maps.html) and then used the result to

207   extract environmental data.

208   **Multicollinearity Analysis Among Variables**

209   Because many environmental variables are spatially correlated and strong correlation between

210   the environmental variables may cause over-fitting and imprecise modeling (Hu & Liu, 2014), we

211   first excluded environmental variables with 0 contribution values using the Maxent Jackknife test

212   (Aguirre-Gutiérrez et al., 2013). Then, we conducted a multicollinearity test in ArcGIS 10.2 to

213   evaluate relationships between the rest of the environmental variables and to eliminate

214   overcounting bias. Finally, we calculated Pearson correlation coefficients using the Band

215   Collection Statistics tool in ArcGIS 10.2 to check the correlations among the 35 bioclimatic

216   variables (Fourcade et al., 2014) and eliminate sampling bias. If a pair of variables were highly

217   correlated ($r \geq 0.8$), only the most ecologically meaningful variables were kept (Aguirre-Gutiérrez

218   et al., 2013). As a result of these analyses, out of the original 35 environmental variables we

219   retained nine for subsequent evaluation.

220   **The Past and Future Climate Scenarios and Years**

221   Climate changes during the late Pleistocene, especially the last glacial–interglacial cycle,

222   greatly impacted vegetation and caused forest types to fluctuate in East Asia (Fang, 1991; Zhou,

223   Qiu & Guo, 1991; Harrison et al., 2001). Because of this, we used three paleoclimate data sets: the

224   Last Interglacial period (LIG, about 120–140 ka), the Last Glacial Maximum (LGM, about 22 ka),

225   and the Mid Holocene (MH, about 6 ka) in the Community Climate System Model four (CCSM4)

226   global climate model (http://www.worldclim.org) to predict possible past distribution areas.

227   CCSM4 is one of the most efficient climate models that can simulate the influence of past and

228   future climatic changes on the distribution of plants (Abdelaal et al., 2019). This model has been

229   already successfully applied in similar studies (Arar et al., 2019; Li, Fan & He, 2020).

230   We applied the Representative Concentration Pathways (RCPs) defined in the IPCC Fifth

231   Assessment Report to predict future conditions. These models better interpret how climate

232 processes work than do the models in the previous four assessment reports (IPCC, 2013). RCPs,

233 including RCP 2.6, RCP4.5, RCP6.0, and RCP 8.5, are potential pathways of radiative forcing

234 values (measured as +2.6, +4.5, +6.0, and +8.5 W/m², respectively) in the year 2100 relative to

235 pre-industrial values. We used four RCP combinations with the CCSM4 climate change modeling

236 data, where 2050 and 2070 use average emissions for the years 2041 to 2060 and 2061 to 2080,

237 respectively. For modeling analyses, we used the RCP 2.6–2050, RCP 2.6–2070, RCP 8.5–2050,

238 and RCP 8.5–2070 combinations with CCSM4 to simulate global climate responses to increased

239 greenhouse gas emissions.

240 ***Model Simulation***

241   Based on distributional data and the selected environmental parameters, we used Maxent for

242 SDM of past, current, and future climate conditions for the whole section, as well as for each

243 species (Phillips et al., 2017). To estimate the capacity of the model, 25% of the data was used for

244 testing, while 75% of the location point data was used for training. SDM was performed using the

245 factors discussed in the previous paragraph, along with occurrence data. The algorithm either ran

246 1,000 iterations of the processes or continued until convergence was reached (threshold, 0.00001).

247 Two methods were utilized to evaluate Maxent performance: the area under the receiver-operating

248 characteristic curve (AUC) (Fielding & Bell, 1997; Babar et al., 2012) and true skill statistic (TSS)

249 (Allouche et al., 2006). AUC is a threshold-independent measurement for assessing model

250 performance (Fielding & Bell, 1997). The value of AUC varies from 0 to 1, with AUC more than

251 0.9 thought to be good prediction (Swets, 1988). Whereas, TSS varies from - 1 and + 1 and takes

252 both omission and commission errors into account. TSS value from 0.70-0.85 indicates good

253 performance, from 0.85-1.00 indicates excellent performance (Luo, Wang & Lyu, 2017). The R

254 package Biomod2 was applied to conduct TSS assessment (Thuiller et al., 2009, 2016).

255   We used the jackknife test to assess the significance of those variables, obtaining a range of

256 values, which we reclassified into four categories of potential suitable habitat: high (> 0.6),

257 moderate (0.4–0.6), low (0.2–0.4), and none (< 0.2) in the final potential species distribution map

258 (Zhang, Zhang & Tao, 2019). Maxent generated a current, three past, and four future climate

259 scenarios to calculate the SDM projections. The distribution shifts between two scenarios were

260 explained by the movement of the central point (the centroid) of the suitable habitat. Suitable

261 habitat changes from one period to the next were estimated by cross-checking the suitable habitat

262 areas in the past and future scenarios against the present distribution area.

263

Results

Model Accuracy and Suitable Areas for Clematis sect. Fruticella

Models for *Clematis* sect. *Fruticella* with a cross-validation AUC of 0.986 and a TSS value of 0.901 (excellent performance) indicated that the Maxent model can accurately predict the location of potential suitable habitat (Figure 2). The potential suitable habitat for the current scenario included Hebei, Inner Mongolia, Shanxi, Shaanxi, Ningxia, Gansu, Qinghai, Sichuan, Xizang, Xinjiang, Yunnan, and Liaoning provinces of China and Mongolia (Figure 2D). Among those, the most suitable areas are concentrated in the Loess Plateau and adjacent areas of northern China. The highly suitable areas cover 238,605 km^2, the moderately suitable areas covers 486,505 km^2, and the least suitable areas encompass 665,699 km^2. The areas with low, medium, and high suitable habitats in the past and future scenarios are in Table S2.

Key Environmental Factors Influencing the Current Habitat

Jackknife results showed that among the proportions of variation of the nine model variables, GloElev (22.9% of variation), UVB4 (22.2%), Precipitation of Coldest Quarter (BIO19, 20.7%), and Mean Temperature of Driest Quarter (BIO9, 18.5%) contributed the greatest weights for the current scenario (Figure 3, Table 1). The cumulative contributions of these four environmental variables (84.3%) were also the most important variables with the highest weights in the seven past and future scenarios (Table S3).

Based on the major variables' response curves, we obtained the thresholds (existence probability > 0.2): GloElev, ranging from 539 to 3620 m; UV-B4, more than 300.5 J/m2/day; all the tested amounts of BIO19, with a peak from 0–47.6 mm and; and BIO9, ranging from -20.7 to 12.3 ℃ (Figure 4).

Suitable Areas Under Climate Changes

The SDM of the LIG (Figure 5B) estimates that southern and western Xinjiang, western and central Inner Mongolia, western Henan, northern Yunnan, southern Xizang, and Central Pakistan, had more suitable habitat (153,522 km^2) than the current distributions. However, the suitable habitat in Xinjiang, Gansu, Ningxia, Inner Mongolia, western Sichuan, Shaanxi, Hebei and eastern Qinghai and Xizang provinces of China decreased significantly, and the habitat in Mongolia was completely lost. In total, there was 730,700 km^2 less suitable habitat in the LIG than there is now. During the LGM, and compared to current amounts, estimated suitable habitat increased by

294   173,431 km², mainly in Gansu, Shaanxi, Shanxi, Henan, Inner Mongolia, Sichuan, and Xinjiang

295   provinces of China, but 174,027 km² was lost, mainly in the northern, northeastern, and

296   southwestern areas of the current suitable habitat (Figure 5C, Table 2). The MH model was similar

297   to that of the LGM, with estimated habitat losses of 137,774 km², mainly in the northern and

298   northeastern distribution areas, the Hengduan Mountains of China, and in Mongolia, but with

299   increases (147,854 km²) in the northern, southern, and western parts of the current habitat.

300   Of the future scenarios, RCP2.6 is based on low levels of greenhouse gas emissions. Maxent

301   estimated that the suitable habitat would increase by 109,356 km² by 2050 under that pathway,

302   mainly in eastern Qinghai-Xizang, western Sichuan, northern Gansu, and Inner Mongolia of China

303   and in Mongolia, but lost suitable habitat of 173,101 km² would occur mainly in Central Xinjiang,

304   western Inner Mongolia, southern Sichuan, and northern Yunnan provinces of China and in

305   Mongolia (Figure 5E, Table 2). By 2070, Maxent estimated that the range of suitable habitat would

306   increase by 124,350 km² mainly in the northern edge of the current habitat, but 132,483 km² of

307   suitable habitat would be lost (Figure 5F, Table 2). Based on high levels of greenhouse gas

308   emissions (RCP 8.5), the estimated habitat in 2050 would increase mainly in the northern margin,

309   but decrease in the western parts of the current suitable habitat (Figure 5G, Table 2). Under the

310   same pathway, Maxent estimated that by 2070 the range of suitable habitat would increase in both

311   the southern and northern margins of the current suitable habitat and decrease mainly in west

312   (Figure 5H).

313   ***Shift of the Distribution Center of Suitable Habitat***

314   The current centroid of suitable habitat was estimated to be in Alxa League, Inner Mongolia

315   (38°14'13"N, 105°13'24"E). However, during the LIG period, the habitat centroid was in northern

316   Ningxia province (40°42'46.8"N, 101°54'32.4"E). This centroid shifted to the southwest during the

317   LGM (37°48'47"N, 105°3'22"E). In the MH, the centroid was very close to its current location

318   (37°58'38"N, 104°49'35"E). Looking to a possible future under RCP 2.6, the centroid will have

319   shifted eastward to central Ningxia Province (38°12'1"N, 106°22'53"E) by 2050, and then would

320   move backward (38°22'23"N, 105°33'31"E) by 2070. Applying RCP 8.5, the centroid is predicted

321   to shift northeast (38°47'19"N, 105°36'35"E) by 2050 and then shift eastward to Ordos, Inner

322   Mongolia (38°40'4"N, 106°47'42"E) by 2070.

323

324

325 **Discussion**

326   The Loess Plateau of China, known by its arid and semi-arid climate, low vegetation

327   coverage, erodible soil, and extensive monsoonal influence, has some of the most severe soil and

328   water loss conditions in the world (Fang et al., 2011; Jiang et al., 2013; Wu et al., 2019). This

329   area's natural vegetation is a key factor controlling soil erosion and stopping desertification

330   (Zheng, 2006; Fang et al., 2011). Species of *Clematis* sect. *Fruticella* members, important

331   components of xerophytic vegetation in China (He, Liu & Xie, 2018), are found over the entire

332   Chinese Loess Plateau and in adjacent arid areas (Wang & Li, 2005a). This study presented a

333   detailed analysis of this native plant taxon's current suitable habitat, as well as its predicted

334   habitat under past and future climate scenarios. Our goal was to provide important insights into

335   the feasibility of using those species for soil fixation in the arid and semi-arid environments of

336   northeast Asia.

337   Our models showed that *Clematis* sect. *Fruticella* could potentially be distributed in a wide

338   range of arid or semi-arid areas in Mongolia and parts of Xinjiang, southeastern Xizang, and

339   southern Sichuan provinces in northern and western China (Figure 2D) where it is currently not

340   found. Moderately and highly suitable habitats predicted by our model are consistent with this

341   section's actual present distribution (725,110 km^2). Because the section's predicted distribution

342   area was broader than its actual distribution area, this study provides more expanded areas for the

343   cultivation of this section's species.

344   When the nine tested variables were run through the jackknife test (Figure 3), GloElev,

345   UVB4, BIO19, and BIO9 were the dominant elements driving the section's potential and current

346   distributions. The GloElev response curve (Figure 4) showed that the estimated suitable

347   elevation for this section is 539 to 3,620 m. This model estimation was highly consistent with,

348   but a little wider, in range compared to the section's actual elevation. From specimen records, the

349   most widely distributed species, *Clematis fruticosa*, occurs at 700 to 2,300 m. The western Loess

350   Plateau species *C. nannophylla* has a wider elevation range, from 1,200 to 3,200 m. The most

351   narrowly distributed species, *C. canescens*, also has a very narrow elevation range (1,200 to

352   1,500 m). The widely distributed species *C. tomentella* often occurs at 1,300 to 2,200 m. Finally,

353   the north Hengduan Mountains species *C. viridis* has the highest elevation range, from 2,700 to

354   3,600 m. Therefore, the actual elevation distribution of the section is 700 to 3,600 m.

355   Non-ionizing solar UV-B radiation (280–315 nm) is an abiotic stress factor for sessile plant

356   species (Nawkar et al., 2013; Blagojevic et al., 2019; Derebe et al., 2019). Too much UV-B

357   exposure damages both cell membranes and DNA and can cause morphological changes (An et

358   al., 2000; Schmitz & Weissenbock, 2003; Kataria & Guruprasad, 2012). However, as a major

359   energy source, plants need low-level UV-B radiation to help regulate growth and development

360   (Blunden & Arndt, 2011). Since *Clematis* sect. *Fruticella* plants are heliophilous, it was no

361   surprise that one of the UV-B factors, UV-B4, was one of the most important contributing

362   factors in the model. It indicated that UV-B radiation must be at least 300.5 J/m^2/day for

363   *Clematis* sect. *Fruticella* plants to thrive. Previous studies showed that long term UV-B exposure

364   may result in smaller leaves and shorter internodes and plant heights (Antonelli et al., 1997;

365   Krizek, Mirecki & Britz, 2006). Compared to other majority number of climbing and often

366   compound-leafed *Clematis* species, the erect shrubby plants of *Clematis* sect. *Fruticella* also

367   have very reduced simple leaves. Perhaps those characters developed as an adaptive response to

368   strong sunlight.

369   A temperature (BIO9) and a precipitation (BIO19) variable in our model each contributed

370   greatly to the predicted distribution of *Clematis* sect. *Fruticella*. (Table 1). They indicated that

371   precipitation during the winter and temperatures during the dry season were important

372   determinants of the section's distribution. Currently, the section's area of distribution is

373   influenced greatly by a monsoonal climate (Wang et al., 2019), in which the coldest and driest

374   season of the year is winter. Plants of *Clematis* sect. *Fruticella* are dormant in winter and their

375   physiological activities are weak. However, a certain amount of precipitation and temperature

376   accumulation in this period are required for dormancy breaking, vegetative bud development,

377   and flower bud differentiation (Xu et al., 2019).

378   Changing climate has affected species distributions and received much attention in recent

379   ecological studies, including those that have shown that some plant species have shifted their

380   distributions drastically during Quaternary climate changes (Lenoir et al., 2008; Qiu, Fu &

381   Comes, 2011). Distributions of many tree and shrub species typically showed latitudinal range

382   shifts in response to glacial movements during the Quaternary (Petit et al., 2003; Ikeda &

383   Setoguchi, 2007; Qiu, Fu & Comes, 2011). However, the estimated suitable habitat centroid of

384   *Clematis* sect. *Fruticella* was very stable in our study. In our models, it shifted only slightly

385 between the LIG era and the years 2050 and 2070, and no patterns of changing elevation were

386 found in those centroid shifts (Figure 6).

387   During the last glaciation, global temperature was 5–12 ℃ lower than they are now and the

388 glacier areas were 8.4 times of the present time in China (Wang & Liu, 2001; Li et al., 2004;

389 Chen, Kang & Liu, 2011). This greatly affected plant distributions. However, our model showed

390 that suitable habitat for *Clematis* sect. *Fruticella* in the LGM did not shrink as much, as might be

391 expected (Figure 5, Table 2). On the contrary, the smallest area of suitable habitat was estimated

392 to be in the LIG period (Figure 5, Table 2), when it was only about half of the current area, but

393 then expanded significantly in LGM. This situation is like those of other reported cold-adapted

394 plant taxa, such as species of *Picea*, *Taxus*, *Tsuga*, and *Quercus* (Li et al., 2013; Liu et al., 2013;

395 Sun et al., 2015; Yu et al., 2015; Du et al., 2017; Zhang et al., 2018), in which low and more

396 stable LGM temperatures created a dispersal opportunity for cold-adapted plant species (Stewart

397 et al., 2009; Kozhoridze et al., 2015). *Clematis* is one of few cosmopolitan genera in the

398 buttercup family, with some species found in subtropical to tropical areas. However, like most of

399 the genera in Ranunculaceae, majority of *Clematis* species occur in temperate zones and are

400 cold-adapted (e.g., sect. *Montana*, sect. *Atragene*, sect. *Meclatis*, and sect. *Fruticella*). Our

401 models confirmed that the LGM's cold climate did not adversely affect *Clematis* sect. *Fruticella*

402 distribution.

403   Study of the depositional sequences of paleosol and loess layers of the Loess Plateau showed

404 that there were five strong summer and four winter monsoon events in the LIG period,

405 demonstrating an unstable climate during that time (Guan et al., 2007). Paleoenvironmental

406 reconstruction of the Loess Plateau implied that both the highest temperature and precipitation

407 amounts in the last 136,000 years occurred during the LIG period (18.1 ℃, maximum mean

408 annual temperature and 1,000 mm maximum mean annual precipitation) (Lu et al., 2007). That

409 unstable and relatively warm, humid climate may have been the main reason that the suitable

410 habitat for *Clematis* sect. *Fruticella* during the LIG period contracted to its smallest area.

411   In addition to the environmental factors discussed above, other factors, such as interspecific

412 competition, may also influence the distribution of *Clematis* sect. *Fruticella*. During the LIG

413 period, the Loess Plateau had mainly forest and forest-steppe vegetation (Cai et al., 2013). Such

414 forest ecosystems would produce extensive shading, thus creating interspecific competition for

415 solar radiation, a distinct minus for *Clematis* sect. *Fruticella*. Another study showed that *C.*

416 *fruticosa*, now common and widely distributed in Loess Plateau, requires outcrossing, even

417 though it is self-compatible (Hou et al., 2016). A forest environment could hinder pollen and

418 fruit migration and prevent long-distance species dispersal. These ecological factors could

419 contribute to the contraction of suitable habitat for *Clematis* sect. *Fruticella* during LIG.

420 Our model suggests that during the transition from the LIG to the LGM, the suitable habitat

421 of *Clematis* sect. *Fruticella* expanded to an area very similar to what is seen today. Thus, the

422 suitable habitat demonstrated stability from the LGM to the future scenarios. No significant area

423 expansion/contraction or latitudinal/altitudinal shifts were detected after the LGM. As the

424 climate changed from warm and humid (LIG) to cold and dry (LGM), the forest ecosystems were

425 then changed into steppe and desert steppe predominantly occupied by *Artemisia* and

426 Chenopodiaceae (Cheng & Jiang, 2011). During that time, the cold and drought tolerances of

427 *Clematis* sect. *Fruticella* facilitated its adaption to the environment and fostered its expanded

428 distribution. To the MH, the climate and vegetation of the Loess Plateau and adjacent areas were

429 like those of the present (Ge & Wei, 2008; Cheng & Jiang, 2011), so the predicted suitable

430 habitat of *Clematis* sect. *Fruticella* remains stable with only minor changes.

431 Distribution ranges of many plant species in the Northern Hemisphere may shift northward

432 or to higher elevations in response to the global warming in the future (Hof et al., 2011; Bai, Wei

433 & Li, 2018; Wang et al., 2019; Zhang, Zhang & Tao, 2019). However, *Clematis* sect. *Fruticella*

434 would likely experience very limited changes in suitable habitat in the future. Although plants of

435 this section are essentially cold adapted, they are also widely adaptable to warm temperatures

436 during summer. Studies have indicated that the semi-arid regions in China will continue to

437 expand, and less precipitation and soil moisture and increased drought frequency may occur

438 because of global warming (Chou et al., 2009; Huang et al., 2019). These changes will not

439 adversely affect the suitable habitat of the drought-resistant *Clematis* sect. *Fruticella*.

440

441 **Conclusions**

442 Investigating the effects of climate change on both plant distribution and plant response

443 mechanisms aids the development of effective conservation strategies and sustainable use of

444 biodiversity. According to our modeling, the predicted current potential range of *Clematis* sect.

445 *Fruticella* was broader than its current distribution range, and the GloElev, UVB4, BIO19, and

446 BIO9 variables most affected this section's distribution. Unlike many other plant taxa, *Clematis*

447 sect. *Fruticella* underwent a significant range contraction during the LIG period, and then an

448 expansion during the LGM to amounts similar to present amounts. Cold, dry, and relatively

449 stable climate, as well as steppe or desert steppe environments may have facilitated the range

450 expansion of this cold-adapted and drought-resistant plant taxon during the LGM. Although

451 climate warming will likely intensify in the future, the suitable habitat of *Clematis* sect.

452 *Fruticella* will not much change. Other factors, such as interspecific competition, human

453 activities, and biological interactions (Liu et al., 2016) that could not be integrated into our

454 modelling, may also affect the section's distribution. The results of our study help us understand

455 distributional dynamics of *Clematis* sect. *Fruticella* and may aid the conservation and sustainable

456 use of these important woody plants in Chinese arid and semiarid areas.

457

458 **Reference**

459 Abdelaal, M.; Fois, M.; Fenu, G.; Bacchetta, G. Using MaxEnt modeling to predict the potential distribution of

460   the endemic plant *Rosa arabica* Crép. in Egypt. *Ecol. Inform.* **2019**, *50*, 68–75.

461 Aguirre-Gutiérrez, J.; Carvalheiro, L.G.; Polce, C.; van Loon, E.E.; Raes, N.; Reemer, M.; Biesmeijer J.C. Fit-

462   for-purpose: species distribution model performance depends on evaluation criteria–Dutch Hoverflies as

463   a case study. *PLoS One* **2013**, *8,* e63708.

464 Allouche, O.; Tsoar, A.; Kadmon, R. Assessing the accuracy of species distribution models: prevalence, kappa

465   and the true skill statistic (TSS). *J. Appl. Ecol.* **2006**, *43*, 1223–1232

466 An, L.Z.; Feng, H.Y.; Tang, X.D.; Wang, X.L. Changes of microsomal membrane properties in spring wheat

467   leaves (*Triticum aestivum* L.) exposed to enhanced ultraviolet-B radiation. *J. Photochem. Photobiol. B,*

468   *Biol.* **2000**, *57,* 60–65.

469 Antonelli, F.; Grifoni, D.; Sabatini, F.; Zipoli, G. Morphological and physiological responses of bean plants to

470   supplemental UV radiation in a Mediterranean climate. *Pl. Ecol.* **1997**, *128,* 127–136.

471 Arar, A.; Tabet, S.; Nouidjem, Y.; Bounar, R.; Chenchouni, H. Projected small-scale range reductions of

472   *Cedrus atlantica* forests due to climate change at the Belezma National Park (Algeria). In: Exploring the

473   Nexus of Geoecology, Geography, Geoarcheology and Geotourism: Advances and Applications for

474   Sustainable Development in Environmental Sciences and Agroforestry Research. Springer: Cham, **2019**;

475   pp. 15–19.

476 Austin, M.P.; Smith, T.M.; Niel, K.P.V.; Wellington, A.B. Physiological responses and statistical models of

477   the environmental niche: a comparative study of two co-occurring eucalyptus species. *J. Ecol.* **2009**, *97*,

478   469–507.

479   Babar, S.; Amarnath, G.; Reddy, C.S.; Jentsch, A.; Sudhakar, S. Species distribution models: ecological

480   explanation and prediction of an endemic and endangered plant species (*Pterocarpus santalinus* L. f.).

481   *Curr. Sci.* **2012**, *102,* 1157–1165.

482   Bai, Y.; Wei, X.; Li, X. Distributional dynamics of a vulnerable species in response to past and future climate

483   change: a window for conservation prospects. *PeerJ* **2018**, *6,* e4287.

484   Barbet-Massin, M.; Jiguet, F.; Albert, C.H.; Thuiller, W. Selecting pseudo-absences for species distribution

485   models: How, where and how many? *Methods Ecol. Evol.* **2012**, *3,* 327–338.

486   Beckmann, M.; Václavík, T.; Manceur, A.M.; Šprtová, L.; Wehrden, H.V.; Welk, E.; Cord, A.F. glUV: A

487   global UV-B radiation dataset for macroecological studies. *Methods Ecol. Evol.* **2014**, *5,* 372–383.

488   Bellard, C.; Bertelsmeier, C.; Leadley, P.; Thuiller, W.; Courchamp, F. Impacts of climate change on the

489   future of biodiversity. *Ecol. Letters,* **2012**, *15,* 365–377.

490   Blagojevic, D.; Lee, Y.; Xie, L.; Brede, D.A.; Nybakken, L.; Lind, O.C.; Tollefsen, K.E.; Salbu, B.; Solhaug,

491   K.A.; Olsen, J.E . No evidence of a protective or cumulative negative effect of UV-B on growth

492   inhibition induced by gamma radiation in Scots pine (*Pinus sylvestris*) seedlings. *Photochem. Photobiol.*

493   *Sci.* **2019**, 18, 1945–1962.

494   Blunden, J.; Arndt, D.S. State of the climate in 2011. *Bull. Am. Meteorol. Soc.* **2012**, *93,* S1–S282.

495   Cai, M.; Wei, M.; Xu, D.; Miao, Y.; Wu, F.; Pan, B. Vegetation and climate changes during three interglacial

496   periods represented in the Luochuan loess-paleosol section, on the Chinese Loess Plateau. *Quat.*

497   *Int.* **2013**, *296,* 131–140.

498   Carpenter, G.; Gillison, A.N.; Winter, J. DOMAIN: a flexible modelling procedure for mapping potential

499   distributions of plants and animals. *Biodivers. Conserv.* **1993**, *2,* 667–680.

500   Carvalho, B.M.; Rangel, E.F.; Ready, P.D.; Vale, M.M. Ecological niche modelling predicts southward

501   expansion of *Lutzomyia* (*Nyssomyia*) *flaviscutellata* (Diptera: Psychodidae: Phlebotominae), Vector of

502   *Leishmania* (*Leishmania*) *amazonensis* in South America, under climate change. *PLoS One* **2015**, *10,*

503   e0143282.

504   Chang, M.C. *Clematis* sect. *Fruticella*. In: Flora Reipublicae Popularis Sinicae, Sinicae Agendae Academiae

505   Sinicae Edita, Ed.; Science Press: Beijing, China, **1980**; Volume 28, pp. 147–156.

506   Chen, D.M.; Kang, H.Z.; Liu, C.J. An overview on the potential Quaternary glacial refugia of plants in China

507   mainland. *Bull. Bot. Res.* **2011**, *31,* 623–632.

508   Cheng, Y.F.; Jiang, W.Y. Vegetation and climate changes since the Last Glacial Maximum in the northern

509   Loess Plateau. *Quat. Sci.* **2011**, *31,* 982–989.

510   Chou, C.; Neelin, J.D.; Chen, C. A.; Tu, J.Y. Evaluating the "rich-get-richer" mechanism in tropical

511   precipitation change under global warming. *J. Clim.* **2009**, *22,* 1982–2005.

512   Derebe, A.D.; Roro, A.G.; Asfaw, B.T.; Ayele, W.W.; Hvoslef-Eide, A.K. Effects of solar UV-B radiation

513   exclusion on physiology, growth and yields of taro (*Colocasia esculenta* (L.)) at different altitudes in

514   tropical environments of Southern Ethiopia. *Sci. Horticul.* **2019**, *256,* 108563.

515   Ding X.L.; Zhang X.; Guo Y.Q.; Liu W.S.; Liu B. Seedling raising and afforestation technology of *Clematis*
516   *canescens*. *Ningxia J. Agri. Fores. Sci. Tech.* **2013**, *54,* 25–33.

517   Doxford, S.W.; Freckleton, R.P. Changes in the large-scale distribution of plants: extinction, colonization and
518   the effects of climate. *J. Ecol.* **2012**, *100,* 519–529.

519   Du, F.K.; Hou, M.; Wang, W.; Mao, K.; Hampe, A. Phylogeography of *Quercus aquifolioides* provides novel
520   insights into the Neogene history of a major global hotspot of plant diversity in south-west China. *J.*
521   *Biogeogr.* **2017**, *44,* 294–307.

522   Fang, H.; Li, Q.; Cai, Q.; Liao, Y. Spatial scale dependence of sediment dynamics in a gullied rolling loess
523   region on the Loess Plateau in China. *Environ. Earth Sci.* **2011**, *64,* 693–705.

524   Fang, J.Q. Lake evolution during the last 30,000 years in China, and its implications for environmental change.
525   *Quat. Res.* **1991**, *36,* 37–60.

526   Fielding, A.H.; Bell, J.F. A review of methods for the assessment of prediction errors in conservation
527   presence/absence models. *Environ. Conserv.* **1997**, *24,* 38–49.

528   Fourcade, Y.; Engler, J.O.; Rödder, D.; Secondi, J. Mapping species distributions with Maxent using a
529   geographically biased sample of presence data: a performance assessment of methods for correcting
530   sampling bias. *PloS One* **2014**, *9,* e97122.

531   Ge Y.G.; Wei, M.J. Palaeo-vegetation and palaeo-environment change of last interglacial period in Xishan
532   Mountain of Beijing. *Geol. Sci. Techn. Inf.* **2008**, *27,* 5–12.

533   Grey-Wilson, C. *Clematis* the genus. Timber Press: Portland, USA, **2000**.

534   Guan, Q.; Pan, B.; Gao, H.; Li, B.; Wang, J.; Su, H. Instability characteristics of the East Asian Monsoon
535   recorded by high-resolution loess sections from the last interglacial (MIS5). *Sci. China Ser. D Earth*
536   *Sci.* **2007**, *50,* 1067–1075.

537   Guo, Y.Q.; Zhang, X.; Liu, W.S.; Liu, B. Forestation of *Clematis canescens* in Miao Erling in Tongxin
538   County. *J. Anhui Agri. Sci.* **2012**, *42,* 16222–16223.

539   Handel-Mazzetti, H. Plantae Sinenses a Dre H. Smith annis 1921–1922, 1924 et 1934 lectae. XXXIII.
540   Ranunculaceae. *Acta Hort. Gotob.* **1939**, *13,* 37–219.

541   Harrison, S.P.; Yu, G.; Takahara, H.; Prentice, I.C. Palaeovegetation: diversity of temperate plants in East
542   Asia. *Nature* **2001**, *413,* 129–130.

543   He, J.; Liu, H.J.; Xie, L. Research advances of *Clematis* sect. *Fruticella* (Ranunculaceae). *J. Nanjing Forest.*
544   *Univ. (Nat. Sci. Ed.)* **2018**, 42, 156–162.

545   Hernandez, P.A.; Graham, C.H.; Master, L.L.; Albert, D.L. The effect of sample size and species
546   characteristics on performance of different species distribution modeling methods. *Ecography* **2006**, *29,*
547   773–785.

548   Hijmans, R.J.; Cameron, S.E.; Parra, J.L.; Jones, P.G.; Jarvis, A. Very high resolution interpolated climate
549   surfaces for global land areas. *Int. J. Climatol.* **2005**, *25,* 1965–1978.

550   Hirzel, A.H.; Helfer, V.; Metral, F. Assessing habitat-suitability models with a virtual species. *Ecol. Model.*
551   **2001**, *145,* 111–121.

552   Hof, C.; Levinsky, I.; Araújo, M.B.; Rahbek, C. Rethinking species' ability to cope with rapid climate
553   change. *Glob. Chang. Biol.* **2011**, *17,* 2987–2990.

554   Hou, Q.Z.; Ren, Y.L.; Wen J.; Zhao, D.G.; Wang, S.Y. Breeding system characters and the adaptive
555   significances of downward orientation flowers in *Clematis fruticosa* Turcz. *Acta Bot. Boreal.-Occident.*
556   *Sin.* **2016**, *36,* 2283–2290

557   Hu, J.; Liu, Y. Unveiling the conservation biogeography of a data-deficient endangered bird species under
558   climate change. *PLoS One* **2014**, *9,* e84529.

559   Huang, J.; Ma, J.; Guan X.; Li, Y.; He, H. Progress in semi-arid climate change studies in China. *Adv. Atmos.*
560   *Sci.* **2019**, *36,* 922–937.

561   IIASA; FAO. Global Agro-ecological Zones (GAEZ v3.0), IIASA, Laxenburg, Austria and FAO, Rome, Italy,
562   2012.

563   Ikeda, H.; Setoguchi, H. Phylogeography and refugia of the Japanese endemic alpine plant, *Phyllodoce*
564   *nipponica* Makino (Ericaceae). *J. Biogeogr.* **2007**, *34,* 169–176.

565   IPCC. Climate Change 2013: The Physical Science Basis. Contribution of Working Group I to the Fifth
566   Assessment Report of the Intergovernmental Panel on Climate Change, Stocker, T.F., Qin, D., Plattner,
567   G.K., Tignor, M., Eds.; Cambridge University Press: Cambridge, United Kingdom and New York, NY,
568   USA, **2013**; pp. 1535, ISBN 978-1-107-05799-1.

569   Jiang, W.; Cheng, Y.; Yang, X.; Yang, S. Chinese Loess Plateau vegetation since the Last Glacial Maximum
570   and its implications for vegetation restoration. *J. Appl. Ecol.* **2013**, *50,* 440–448.

571   Johnson M. Släktet Klematis. Magnus Johnson Plantskola AB: Södertälje, Sweden, **1997**.

572   Kataria, S.; Guruprasad, K.N. Solar UV-B and UV-A/B exclusion e□ects on intraspecific variations in crop
573   growth and yield of wheat varieties. *Field Crops Res.* **2012**, *125,* 8–13.

574   Konowalik, K.; Proćków, M.; Proćków, J. Climatic niche of *Selinum alatum* (Apiaceae, Selineae), a new
575   invasive plant species in Central Europe and its alterations according to the climate change scenarios:
576   Are the European mountains threatened by invasion? *PLoS One* **2017**, *12,* e0182793.

577   Kozhoridze, G.; Orlovsky, N.; Orlovsky, L.; Blumberg, D.G.; Golan-Goldhirsh, A. Geographic distribution
578   and migration pathways of *Pistacia*–present, past and future. *Ecography* **2015**, *38,* 1141–1154.

579   Krizek, D.T.; Mirecki, R.M.; Britz, S.J. Inhibitory e□ects of ambient levels of solar UV-A and UV-B radiation
580   on growth of cucumber. *Physiol. Pl.* **2006**, *100,* 886–893.

581   Lehtonen, S.; Christenhusz, M.J.; Falck, D. Sensitive phylogenetics of *Clematis* and its position in
582   Ranunculaceae. *Bot. J. Linn. Soc.* **2016**, *182,* 825–867.

583   Lenoir, J.; Gégout, J.C.; Marquet, P.A.; de Ruffray, P.; Brisse, H. A significant upward shift in plant species
584   optimum elevation during the 20th century. *Science* **2008**, *320,* 1768–1771.

585 Li, J.; Fan, G.; He, Y. Predicting the current and future distribution of three *Coptis* herbs in China under
586   climate change conditions, using the MaxEnt model and chemical analysis. *Sci. Total Environ.* **2020**,
587   *698,* 134141.

588 Li J.J.; Shu, Q.; Zhou, S.Z.; Zhao, Z.J.; Zhang, J.M. Review and prospects of Quaternary glaciation research in
589   China. *J. Glaciol. Geocryol.* **2004**, *26,* 235–243.

590 Li, L.; Abbott, R.J.; Liu, B.; Sun, Y.; Li, L.; Zou, J.; Liu, J. Pliocene intraspecific divergence and
591   Plio-Pleistocene range expansions within *Picea likiangensis* (Lijiang spruce), a dominant forest tree of
592   the Qinghai-Tibet Plateau. *Mol. Ecol.* **2013**, *22,* 5237–5255.

593 Li, W.; Shi, M.; Huang, Y.; Chen, K.; Sun, H.; Chen, J. Climatic change can influence species diversity
594   patterns and potential habitats of Salicaceae plants in China. *Forests* **2019**, *10,* 220.

595 Li, X.; Wang, Y. Applying various algorithms for species distribution modelling. *Integr. Zool.* **2013**, *8,* 124–
596   135.

597 Liu M.; Zheng R.; Bai S.L.; Qing Y.; Yan W.; Jia X.W. Seasonal dynamics of arbuscular mycorrhizal fungal
598   community in the rhizosphere of *Clematis fruticosa* in the Daqingshan Mountains, Inner Mongolia. *Acta*
599   *Bot. Boreal.-Occident. Sin.* **2016**, *36,* 1891–1899.

600 Liu, J.; Möller, M.; Provan, J.; Gao, L.M.; Poudel, R.C.; Li, D.Z. Geological and ecological factors drive
601   cryptic speciation of yews in a biodiversity hotspot. *New Phytol.* **2013**, *199,* 1093–1108.

602 Liu, Y.N.; Wang, L.H.; Zhang, L.J.; Han, R.S.; Zhang, G.S. Physiological response of *Clematis fruticosa*
603   under water stress. *Nor. Horticul.* **2014**, *17,* 71–74.

604 Liu, Y.Y.; van Dijk, A.I.J.M.; McCabe, M.F.; Evans, J.P.; de Jeu, R.A.M. Global vegetation biomass change
605   (1988–2008) and attribution to environmental and human drivers, *Glob. Ecol. Biogeogr.* **2013**, *22,* 692–
606   705.

607 Lu, H.Y.; Wu, N.Q.; Liu, K.B.; Jiang, H.; Liu, T.S. Phytoliths as quantitative indicators for the reconstruction
608   of past environmental conditions in China II: palaeoenvironmental reconstruction in the Loess Plateau.
609   *Quat. Sci. Rev.* **2007**, *26,* 759–772.

610 Luo, M.; Wang, H.; Lyu, Z. Evaluating the performance of species distribution models Biomod2 and MaxEnt
611   using the giant panda distribution data. *J. Appl. Ecol.*, **2017**, *28,* 4001–4006.

612 Maestre, F.T.; Quero, J.L.; Gotelli, N.J.; Escudero, A.; Ochoa, V.; Delgado-Baquerizo, M.; García-Palacios, P.
613   Plant species richness and ecosystem multifunctionality in global drylands. *Science* **2012**, *335,* 214–218.

614 Matías, L.; Linares, J.C.; Sánchez-Miranda, Á.; Jump, A.S. Contrasting growth forecasts across the
615   geographical range of Scots pine due to altitudinal and latitudinal differences in climatic
616   sensitivity. *Glob. Chang. Biol.* **2017**, *23,* 4106–4116.

617 Miller, J. A. Species distribution models: Spatial autocorrelation and non-stationarity. *Prog. Phys. Geogr.*
618   **2012**, *36,* 681–692.

619 Mitchell, T.D.; Jones, P.D. An improved method of constructing a database of monthly climate observations
620   and associated high-resolution grids. *Int. J. Climatol.* **2005**, *25,* 693–712.

621 Mohammadi, S.; Ebrahimi, E.; Moghadam, M.S.; Bosso, L. Modelling current and future potential
622   distributions of two desert jerboas under climate change in Iran. *Ecol. Inform.* **2019**, *52,* 7–13.

623 Nawkar, G.M.; Maibam, P.; Park, J.H.; Sahi, V.P.; Lee, S.Y.; Kang, C.H. UV-induced cell death in plants. *Int.*
624   *J. Mol. Sci.* **2013**, *14,* 1608–1628.

625 New, M.; Hulme, M.; Jones, P. Representing twentieth-century space-time climate variability. Part I:
626   Development of a 1961–1990 mean monthly terrestrial climatology. *J. Clim.* **1999**, *12,* 829–856.

627 Parmesan, C.; Yohe, G. A globally coherent fingerprint of climate change impacts across natural
628   systems. *Nature* **2003**, *421,* 37.

629 Peterson, A.T.; Soberón, J.; Pearson, R.G.; Anderson, R.P.; Martínez-Meyer, E.; Nakamura, M.; Araújo, M.B.
630   Ecological niches and geographic distribution. *Monogr. Popul. Biol.* **2011**, *49,* 328.

631 Petit, R.J.; Aguinagalde, I.; de Beaulieu, J.L.; Bittkau, C.; Brewer, S.; Cheddadi, R.; Ennos, R.; Fineschi,
632   S.; Grivet, D.; Lascoux, M.; Mohanty, A.; Müller-Starck, G.; Demesure-Musch, B.; Palmé, A.; Martín,
633   J.P.; Rendell, S.; Vendramin, G.G. Glacial refuges: hotspots but not melting pots of genetic diversity.
634   *Science* **2003**, 300, 1563–1565.

635 Phillips, S.J.; Anderson, R.P.; Dudík, M.; Schapire, R.E.; Blair, M.E. Opening the black box: An open-source
636   release of Maxent. *Ecography* **2017**, *40,* 887–893.

637 Phillips, S.J.; Anderson, R.P.; Schapire, R.E. Maximum entropy modeling of species geographic
638   distributions. *Ecol. Model.* **2006**, *190,* 231–259.

639 Pio, D.V.; Engler, R.; Linder, H.P.; Monadjem, A.; Cotterill, F.P.D; Taylor, P.J.; Schoeman, M.C.; Price,
640   B.W.; Villet, M.H.; Eick, G.; Salamin, N.; Guisan, A. Climate change effects on animal and plant
641   phylogenetic diversity in southern Africa. *Glob. Chang. Biol.* **2014**, *20,* 1538–1549.

642 Prantl, K. *Clematis*. Beträge zur Morphologie und Systematik der Ranunculaceen. *Bot. Jahrb.* **1888**, *9,* 325–
643   373.

644 Qin, H.; Dong, G.; Zhang, Y.; Zhang, F.; Wang, M. Patterns of species and phylogenetic diversity of *Pinus*
645   *tabuliformis* forests in the eastern Loess Plateau. *For. Ecol. Manage* **2017**, *394,* 42–51.

646 Qiu, Y.X.; Fu, C.X.; Comes, H.P. Plant molecular phylogeography in China and adjacent regions: Tracing the
647   genetic imprints of Quaternary climate and environmental change in the world's most diverse temperate
648   flora. *Mol. Phylogenet. Evol.* **2011**, *59,* 225–244.

649 Schmitz, R.; Weissenbock, G. Contribution of phenolic compounds to the UV-B screening capacity of
650   developing barley primary leaves in relation to DNA damage and repair under elevated UV-B levels.
651   *Photochem.* **2003**, *64,* 243–255.

652 Stewart, J.R.; Lister, A.M.; Barnes, I.; Dalén, L. Refugia revisited: individualistic responses of species in space
653   and time. *Proc. Biol. Sci.* **2009**, *277,* 661–671.

654 Sun, Y.; Li, L.; Li, L.; Zou, J.; Liu, J. Distributional dynamics and interspecific gene flow in *Picea likiangensis*
655   and *P. wilsonii* triggered by climate change on the Qinghai-Tibet Plateau. *J. Biogeogr.* **2015**, *42,* 475–
656   484.

657   Swets, J.A. Measuring the accuracy of diagnostic systems. *Sciences* **1988**, *240,*1285–1293.

658   Tamura, M. *Archiclematis & Clematis*. In Die Natürlichen Pflanzenfamilien, 2rd ed.; Hiepko, P., Ed.; Duncker
659   & Humblot: Berlin, Germany, **1995**; Volume 17, pp. 366–387.

660   Tamura, M. Morphology, ecology and phylogeny of the Ranunculaceae. VII. *Sci. Rep. Osaka Univ.* **1967**, *16,*
661   21–43.

662   Thuiller, W.; Lafourcade, B.; Engler, R.; Araújo, M.B. Biomod: A platform for ensemble forecasting of
663   species distributions. *Ecography*, **2009**, *32,* 369－373.

664   Thuiller, W.; Georges, D.; Engler, R.; Breiner, F.; Georges, M.D.; Thuiller, C.W. Package 'biomod2'. Species
665   distribution modeling within an ensemble forecasting framework. **2016**, https://CRAN. R-project.
666   org/package= biomod2.

667   Walck, J.L.; Hidayati, S.N.; Dixon, K.W.; Thompson, K.E.N.; Poschlod, P. Climate change and plant
668   regeneration from seed. *Glob. Chang. Biol.* **2011**, *17,* 2145–2161.

669   Wang, D.; Cui, B.; Duan, S.; Chen, J.; Fan, H.; Lu, B.; Zheng, J. Moving north in China: The habitat of
670   *Pedicularis kansuensis* in the context of climate change. *Sci. Total Environ.* **2019**, *97,* 133979.

671   Wang, H.; Lu, H.; Zhang, H.; Yi, S.; Gu, Y.; Liang, C. Grass habitat analysis and phytolith-based quantitative
672   reconstruction of Asian monsoon climate change in the sand-loess transitional zone, northern China.
673   *Quat. Res.* **2019**, *92,* 519–529.

674   Wang, R.; Li, Q.; He, S.; Liu, Y.; Wang, M.; Jiang, G. Modeling and mapping the current and future
675   distribution of *Pseudomonas syringae* pv. *actinidiae* under climate change in China. *PloS One* **2018**, *13,*
676   e0192153.

677   Wang, W.T. A revision of *Clematis* sect. *Clematis* (Ranunculaceae). *Acta Phytotax. Sin.* **2003**, *41,* 1–62.

678   Wang, W.T.; Li, L.Q. A revision of *Clematis* sect. *Fruticella* (Ranunculaceae). *Acta. Phytotax. Sin.* **2005a**, *43,*
679   193–209.

680   Wang, W.T.; Li, L.Q. A new system of classification of the genus *Clematis* (Ranunculaceae). *Acta. Phytotax.*
681   *Sin.* **2005b**, *43,* 431–488.

682   Wang, Z.T.; Liu, C.H. Geographical characteristics of the distribution of glaciers in China. *J. Glaciol.*
683   *Geocryol.* **2001**, *23,* 231–237.

684   Wu, J.; Miao, C.; Duan, Q.; Lei, X.; Li, X.; Li, H. Dynamics and attributions of baseflow in the semiarid Loess
685   Plateau. *J. Geophys. Res. Atmos.* **2019**, *124,* 3684–3701.

686   Xu, D.; Zhuo, Z.; Wang, R.; Ye, M.; Pu, B. Modeling the distribution of *Zanthoxylum armatum* in China with
687   MaxEnt modeling. *Glob. Ecol. Conserv.* **2019**, *19,* e00691.

688   Xu, Z. P.; Zhang, J.Q.; Wan, T.; Cai, P.; Yi, W.D. Study on the history distribution pattern of *Gymnocarpos*
689   *przewalskii* and refuge area. *Acta Bot. Bor.-Occid. Sin.* **2017**, *37,* 2074–2081.

690   Yu, H.; Zhang, Y.; Liu, L.; Qi, W.; Li, S.; Hu, Z. Combining the least cost path method with population
691   genetic data and species distribution models to identify landscape connectivity during the late
692   Quaternary in Himalayan hemlock. *Ecol. Evol.* **2015**, *5,* 5781–5791.
693   Yu, H.R.; Li, Q.F.; Jia, Y.S.; He, Y.M. Study on dormancy and germination characteristics of four kinds of
694   shrub plant seeds. *Nor. Horticul.* **2018**, *22,* 88–93.
695   Zhang, A.P.; Wang, Y.; Xiong, Q.L.; Wu, X.G.; Sun, X.M.; Huang, Y.M.; Zhang, L.; Pan, K.W. Distribution
696   changes and refugia of three spruce taxa since the last interglacial. *J. Appl. Ecol.* **2018**, *29,* 2411–2421.
697   Zhang, K.; Yao, L.; Meng, J.; Tao, J. Maxent modeling for predicting the potential geographical distribution of
698   two peony species under climate change. *Sci. Total Environ.* **2018**, *634,* 1326–1334.
699   Zhang, K.; Zhang, Y.; Tao, J. Predicting the potential distribution of *Paeonia veitchii* (Paeoniaceae) in China
700   by incorporating climate change into a Maxent model. *Forests* **2019**, *10,* 190.
701   Zhang, M.G.; Zhou, Z.K.; Chen, W.Y.; Slik, J.F.; Cannon, C.H.; Raes, N. Using species distribution modeling
702   to improve conservation and land use planning of Yunnan, China. *Biol. Conserv.* **2012**, *153,* 257–264.
703   Zhen, H.Y.; Liu, Y. Study on seeds biological characteristics of 2 ornamental plant of sect. *Fruticella*. *Seed*
704   **2010**, *29,* 42–44.
705   Zheng, F.L. Effect of vegetation changes on soil erosion on the Loess Plateau. *Pedosphere* **2006**, *16,* 420–427.
706   Zhou, Y.; Qiu, G.; Guo, D. Changes of permafrost in China during the Quaternary. In Quaternary Geology and
707   Environment in China, Liu, T., Ed.; Science Press: Beijing, China, **1991**; pp. 86–94.

Figure 1

Distribution of *Clematis* sect. *Fruticella* in China and Mongolia.
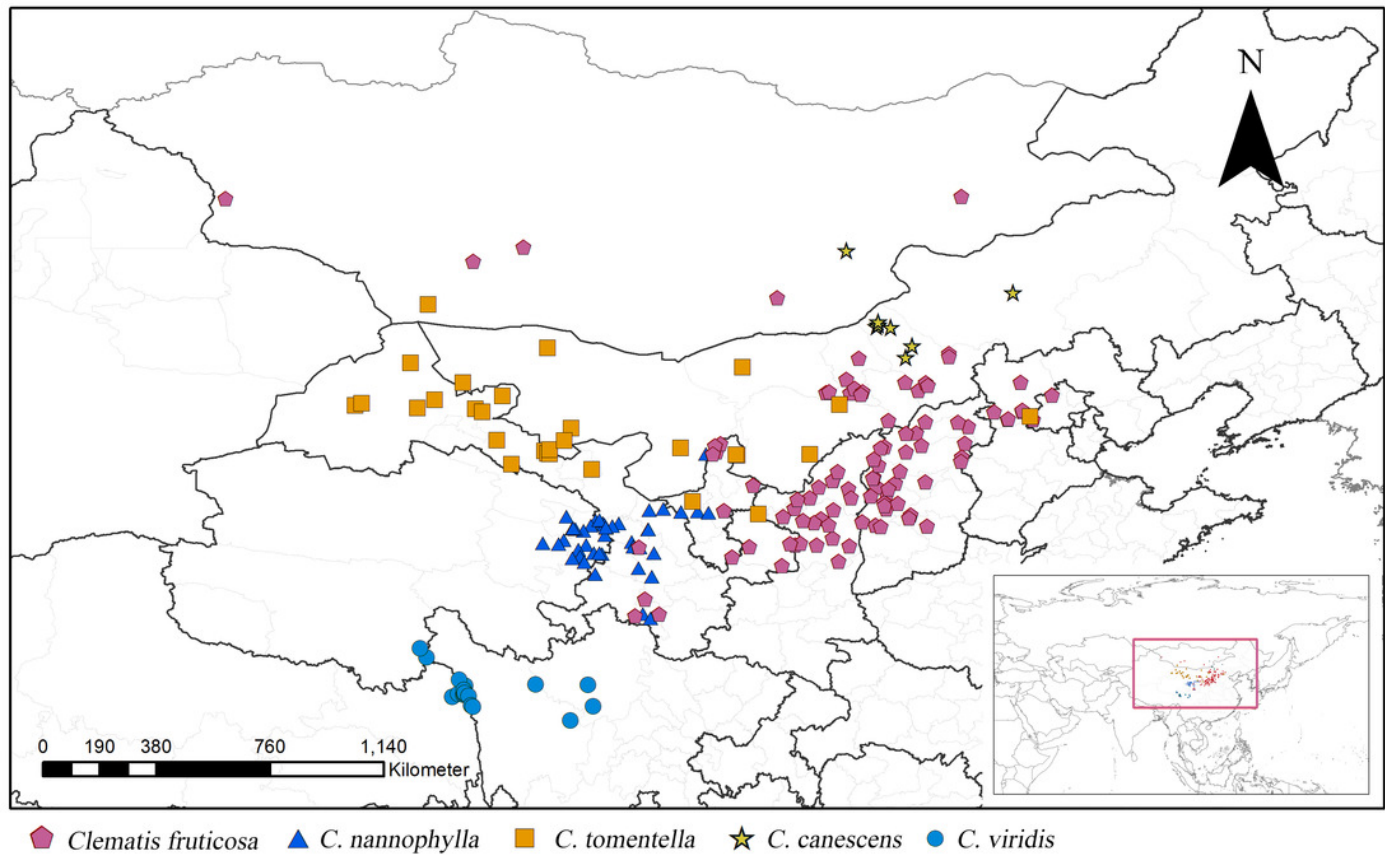
Figure 2

Potential suitable distribution areas for *Clematis* sect. *Fruticella* predicted using Maxent modeling of eight scenarios.

(A) Last interglacial (B) Last glacial Maximum. (C) Mid Holocene. (D) Current. (E) Year of 2050 (under RCP2.6). (F) Year of 2070 (under RCP2.6). (G) Year of 2050 (under RCP8.5). (H) Year of 2070(under RCP8.5). RCP: representative concentration pathway.
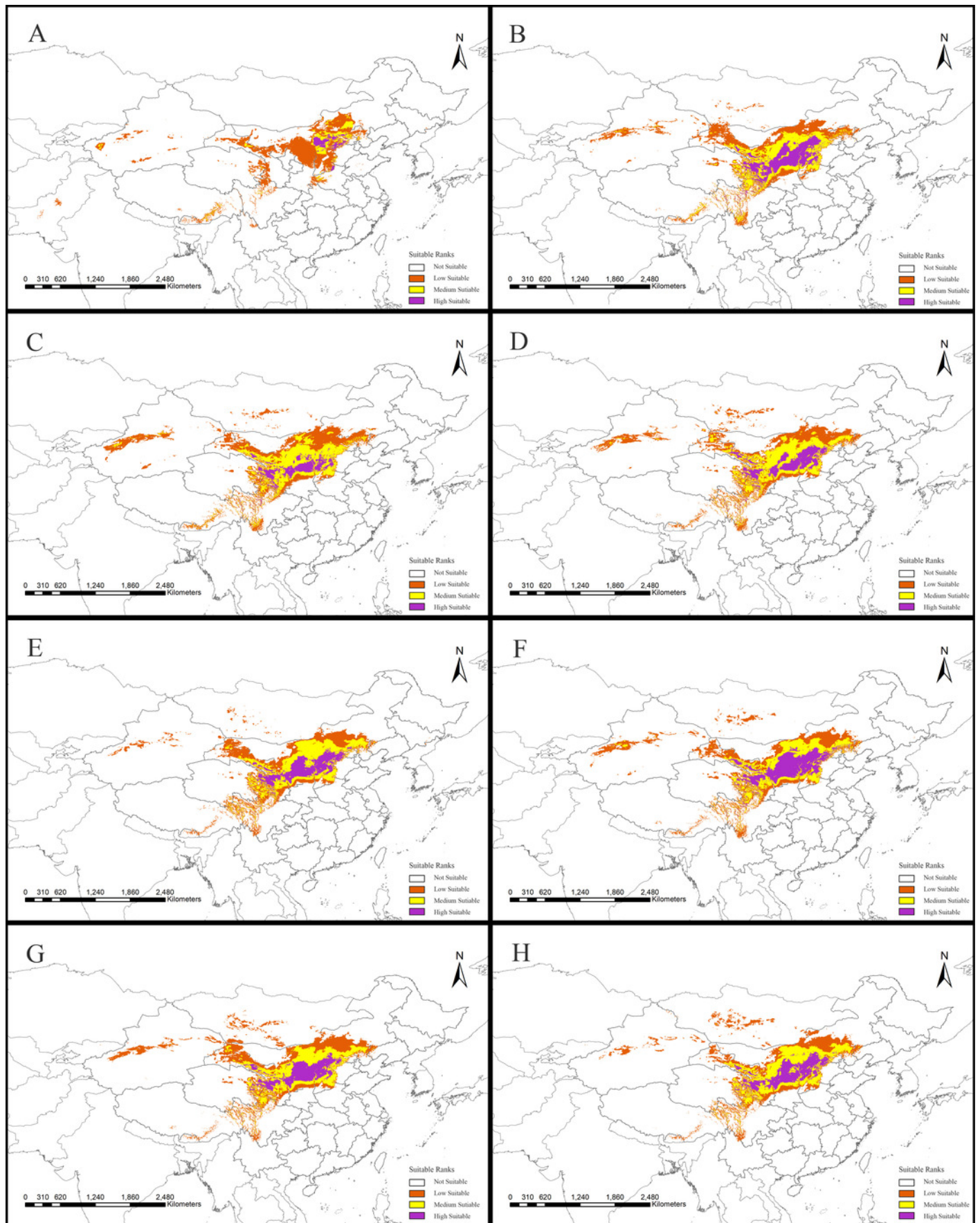
Figure 3

Jackknife test results showing the relative importance (training gain) of the nine selected environmental variables for *Clematis* sect. *Fruticella*.
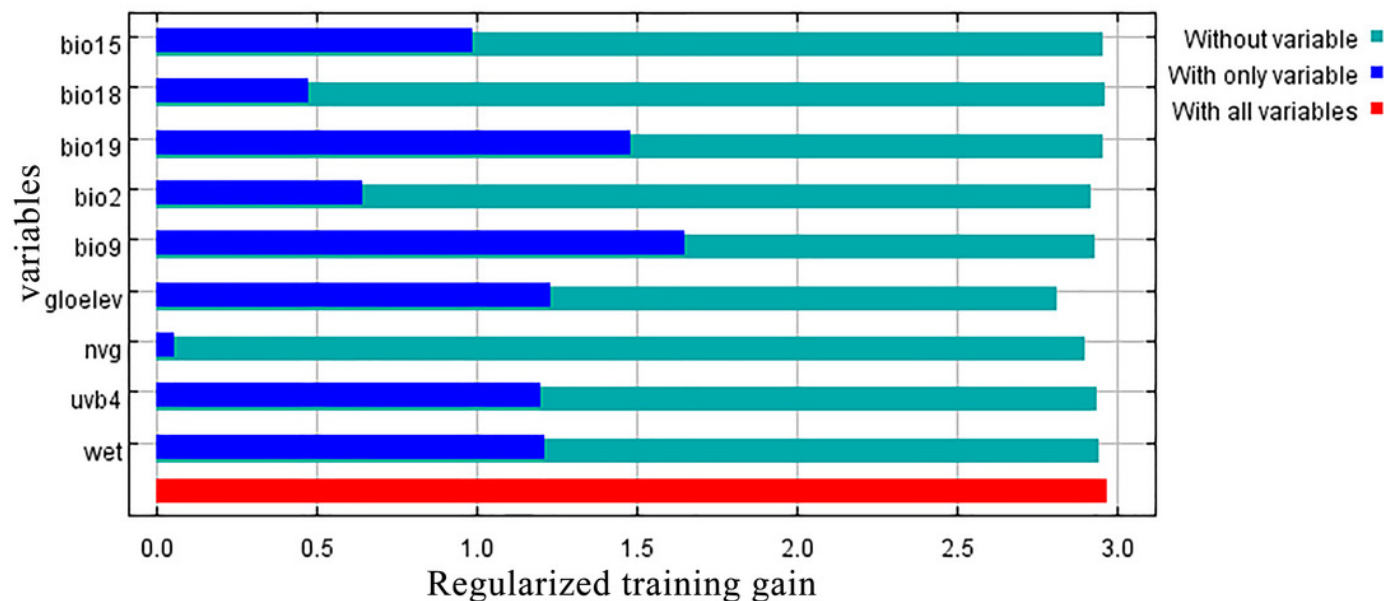
Figure 4

Response curves for the four most important environmental predictors in the *Clematis* sect. *Fruticella* distribution model.

(A) Elevation. (B) Mean UV-B of Lowest Month. (C) Precipition of Coldest Quarter. (D) Mean Temperature of Driest Quarst.
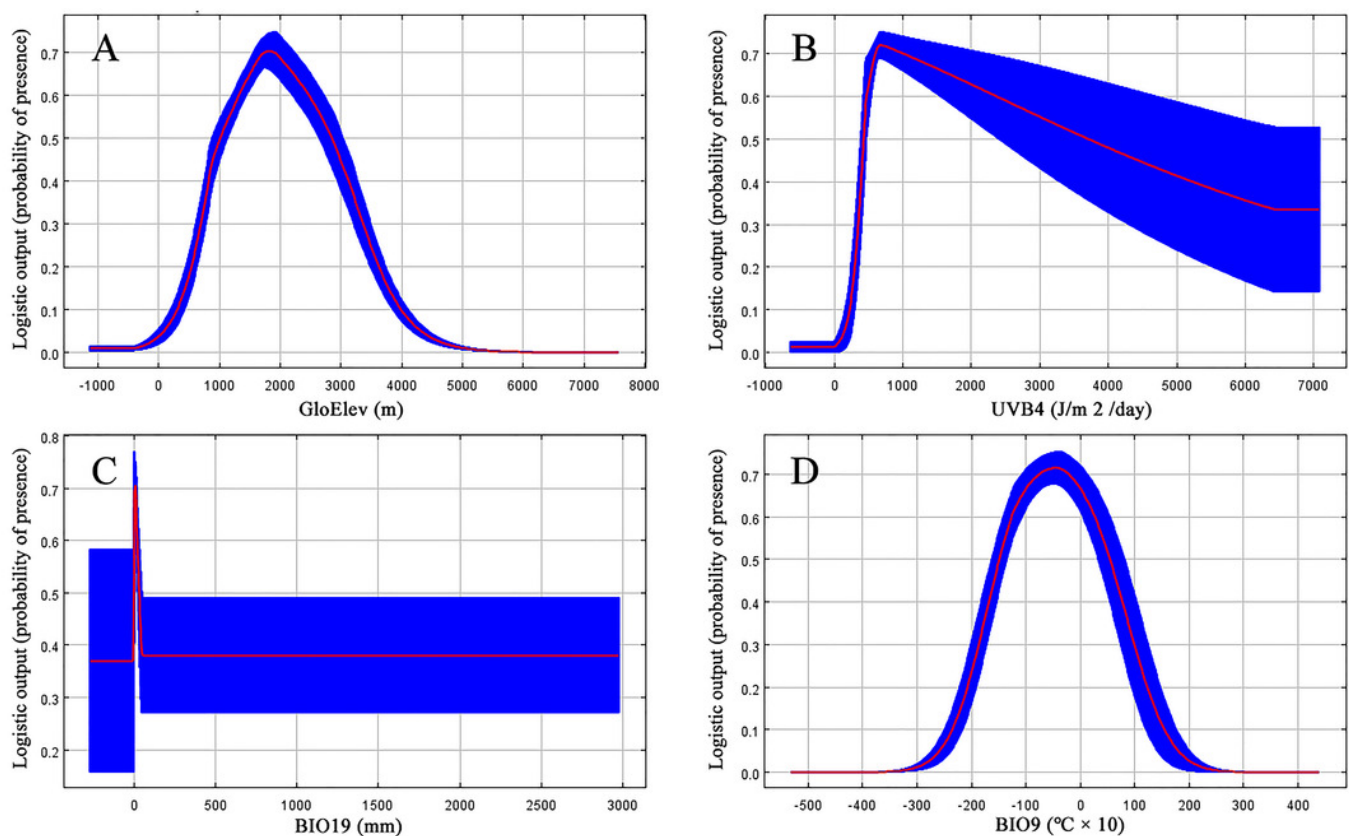
Figure 5

Species distribution models (SDMs) of *Clematis* sect. *Fruticella*.

Models B through H reflect habitat differences compared to the current model A. (A) Current. (B) Last Interglacial. (C) Last Glacial Maximum. (D) Mid Holocene. (E) Year of 2050 (under RCP2.6). (F) Year of 2070 (under RCP2.6). (G) Year of 2050 (under RCP8.5). (H) Year of 2070(under RCP8.5). RCP: representative concentration pathway.
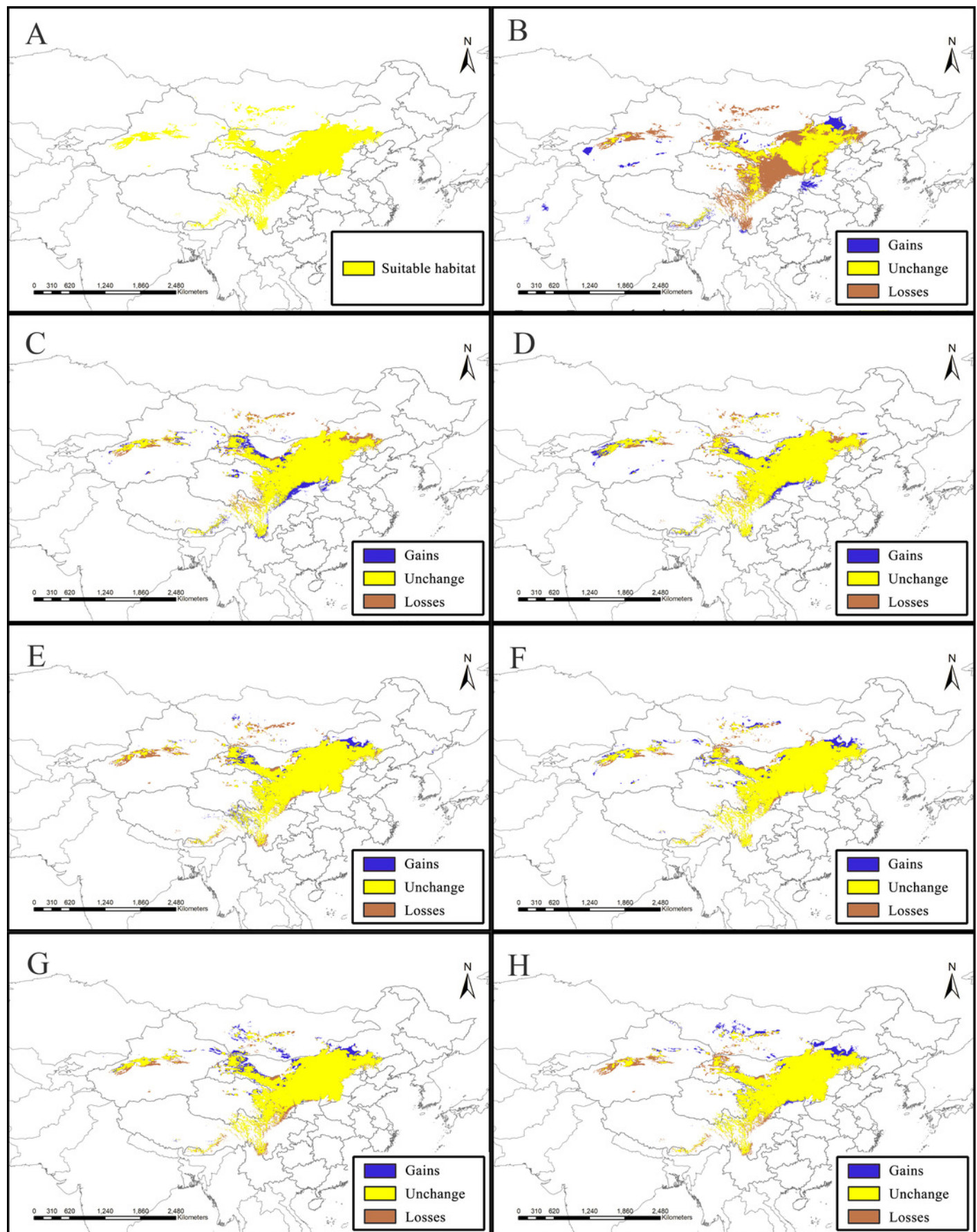
Figure 6

Core distributional shifts of *Clematis* sect. *Fruticella* under the four future and three past climate scenarios.

The distribution centroids are all in northern China. RCP: representative concentration pathway.
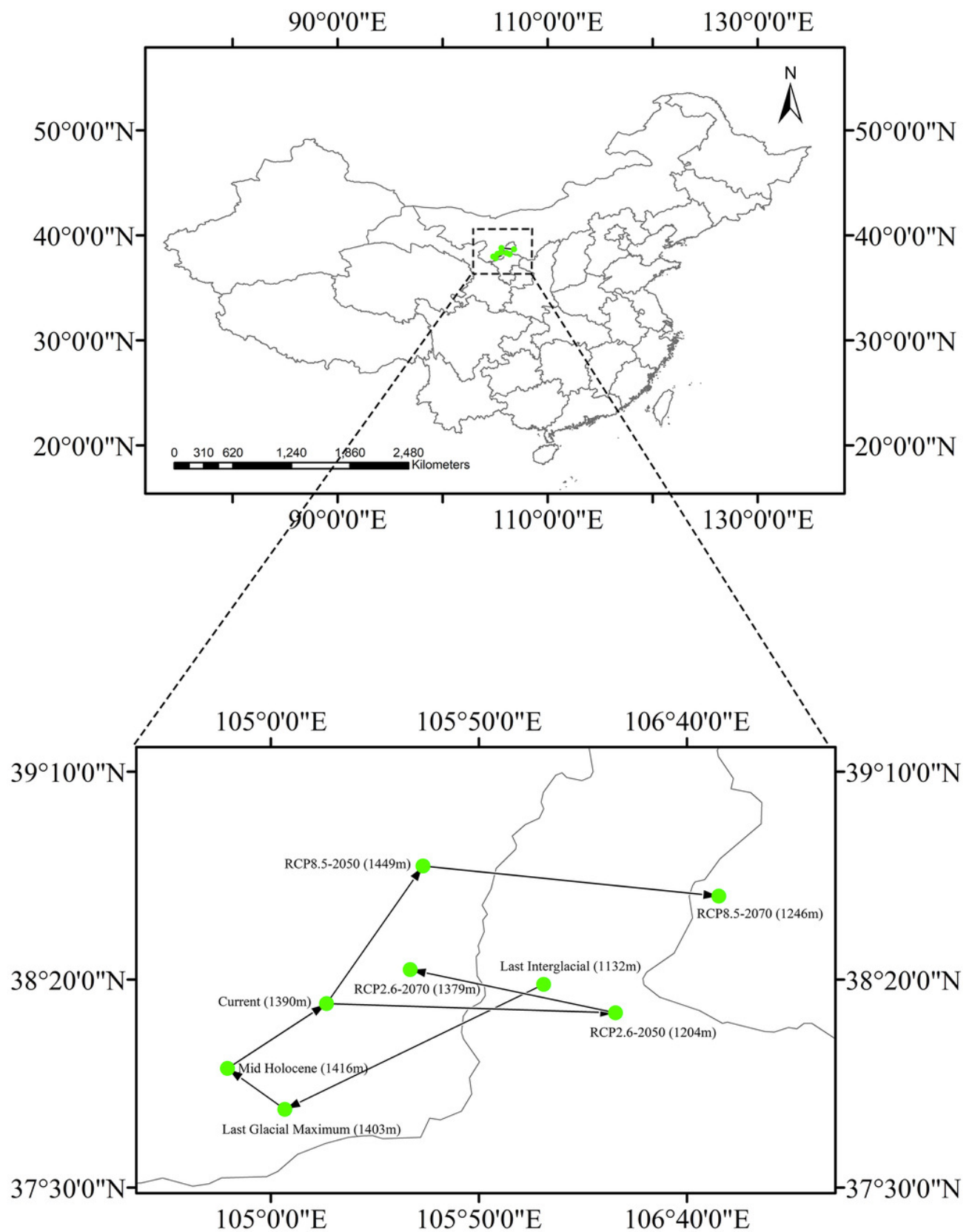
Percentage contributions and permutation importance of the variables included in the Maxent models for *Clematis* sect. *Fruticella*.

1 **Table 1:**

2 **Percentage contributions and permutation importance of the variables included in the Maxent models for *Clematis* sect.**

3 ***Fruticella.***

Environmental Variables	Resolution	Unit	Contribution (%)
Elevation (GloElev)	$30'' \times 30''$	m	22.9
Mean UV-B of Lowest Month (UVB4)	$15' \times 15'$	J/m^2/day	22.2
Precipitation of Coldest Quarter (BIO19)	$2.5' \times 2.5'$	mm	20.7
Mean Temperature of Driest Quarter (BIO9)	$2.5' \times 2.5'$	℃ × 10	18.5
barren/very sparsely vegetated land (NVG)	$5' \times 5'$		7.5
Mean Diurnal Range (Mean of monthly (max − min) temp) (BIO2)	$2.5' \times 2.5'$	℃ × 10	2.8
Wet days (WET)	$30' \times 30'$	d.	2.2
Precipitation of Warmest Quarter (BIO18)	$2.5' \times 2.5'$	mm	2
Precipitation Seasonality (Coefficient of Variation) (BIO15)	$2.5' \times 2.5'$	mm	1.1

Dynamic changes in the distribution area for *Clematis* sect. *Fruticella* under four future and three past climate scenarios compared to the current suitable habitat area.

1 **Table 2:**
2 **Dynamic changes in the distribution area for *Clematis* sect. *Fruticella* under four**
3 **future and three past climate scenarios compared to the current suitable habitat area.**

Scenarios	Increased(km^2)	Unchanged(km^2)	Decreased(km^2)
Last interglacial	153,522.601	660,109.5024	730,700.3814
Last Glacial Maximum	173,431.2386	121,6782.014	174,027.8697
Mid Holocene	147,854.6056	125,3035.203	137,774.6803
[1]RCP2.6-2050	109,356.1992	121,7708.362	173,101.5214
RCP2.6-2070	124,350.4807	125,8326.379	132,483.5045
RCP8.5-2050	146,755.5483	124,6927.585	143,882.2986
RCP8.5-2070	123,800.952	1,200,798.581	190,011.3027

4 [1]RCP:representative concentration pathway